

**Received:** 23 January, 2025  
**Accepted:** 01 February, 2025  
**Published:** 03 February, 2025

**\*Corresponding author:** Lakshmi N Sridhar, Chemical Engineering Department, University of Puerto Rico, Mayaguez PR 00681-9046, Puerto Rico, E-mail: lakshmin.sridhar@upr.edu

**Keywords:** Circadian; Dopamine; Bifurcation; Optimal control

**Copyright License:** © 2025 Sridhar LN. This is an open-access article distributed under the terms of the Creative Commons Attribution License, which permits unrestricted use, distribution, and reproduction in any medium, provided the original author and source are credited.

<https://www.clinsurgroup.us>



## Review Article

# Analysis and Control of the Dopamine Circadian Rhythms Model

Lakshmi N Sridhar\*

Chemical Engineering Department, University of Puerto Rico, Mayaguez PR 00681-9046, Puerto Rico

## Abstract

**Background:** The high nonlinearity of the dopamine circadian rhythms model is seen in the presence of limited cycles that disrupt the circadian rhythms. Limit Cycles originate from Hopf bifurcation points. Bifurcation analysis and Multiobjective nonlinear model predictive control are performed on the dopamine circadian rhythms model.

**Methods:** The MATLAB software MATCONT was used to perform the bifurcation analysis. The Multi-objective Nonlinear Model Predictive Control was performed using the optimization language PYOMO.

**Results:** The Bifurcation analysis reveals Hopf Bifurcation points that produce limit cycles. To eliminate the rhythm disturbing limit cycles the bifurcation parameter is multiplied by an activation factor involving the tanh function. The nonlinearity of the dopamine circadian rhythms model also causes spikes in the control profiles when multiobjective nonlinear model predictive control calculations are performed. The spikes are also eliminated when the control variable is multiplied by the same activation factor.

**Conclusion:** The dopamine circadian rhythms model is shown to have two Hopf bifurcations, which cause limit cycles that can disrupt the circadian rhythms. An activation factor involving the tanh function eliminates the limit cycle causing Hopf bifurcations. This activation factor also removes the spikes that occur in the control profile.

## Background and introduction

Graybiel and Kimura [1] researched the basal ganglia in adaptive motor control. Vitaterna, et al. [2] studied the differential regulation of mammalian period genes and circadian rhythmicity by cryptochromes 1 and 2. Van der Horst, et al. [3] demonstrated that mammalian cry1 and cry2 are essential for the maintenance of circadian rhythms. Strogatz [4] explored the onset of synchronization in coupled oscillators. Shearman, et al. [5] discussed how the molecular loops interact in the mammalian circadian clock. Abarca, et al. [6] showed that Cocaine sensitization and reward are under the influence of circadian genes and rhythm. Preitner, et al. [7] demonstrated that the orphan nuclear receptor rev-erb $\alpha$  controls circadian transcription within the positive limb of the mammalian circadian oscillator.

Lotharius and Brundin [8] investigated the pathogenesis of Parkinson's disease with regard to dopamine vesicles and alpha-synuclein. Oleksiak, et al. [9] studied the variation in gene expression within and among natural populations. Boeuf, et al. [10] investigated the individual variation of adipose gene expression and identified covariate genes by cDNA microarrays. Forger and Peskin [11] provided a detailed predictive model of the mammalian circadian clock. Leloup and Goldbeter [12] came up with a detailed computational model for the mammalian circadian clock. Sato, et al. [13] demonstrated a functional genomics strategy that reveals rora as a component of the mammalian circadian clock. Castaneda, et al. [14] discussed the circadian rhythms of dopamine, glutamate, and GABA in the striatum and nucleus accumbens of the awake rat.



Kienast and Heinz [15] conducted research on Dopamine in the diseased brain. Sigal, et al. [16] discussed the Variability and memory of protein levels in human cells. Hong, et al. [17] showed a strategy for robust temperature compensation of circadian rhythms. McClung [18] researched the effect of circadian genes, rhythms, and the biology of mood disorders. Sleipness, et al. [19] discussed the diurnal differences in dopamine transporter and tyrosine hydroxylase levels in rat brain: Dependence on the suprachiasmatic nucleus. Hampp, et al. [20] investigated the regulation of monoamine oxidase by circadian clock components.

Liu, et al. [21] investigated the redundant function of *rev-erb $\alpha$*  and *\beta* and the non-essential role of *bmal1* cycling in the transcriptional regulation of intracellular circadian rhythms. Hood, et al. [22] demonstrate that Endogenous dopamine regulates the rhythm of expression of the clock protein *per2* in the rat dorsal striatum via daily activation of d2 dopamine receptors. Ripperger, et al. [23] investigated the daily rhythm of mice. Gravotta, et al. [24] showed that the depletion of dopamine using intracerebroventricular 6-hydroxydopamine injection disrupts normal circadian wheel-running patterns and *period2* expression in the rat forebrain. Bugge, et al. [25] show that the *Rev-erb $\alpha$*  and *rev-erb $\beta$*  co-ordinately protect the circadian clock and normal metabolic function. Solt, et al. [26] demonstrated a method to regulate circadian behavior and metabolism by synthetic *rev-erb* agonists. While Ikeda, et al. [27] discovered the molecular mechanism that regulates the 24-hour rhythm of dopamine d3 receptor expression in mouse ventral striatum.

Karatsoreos [28] studied the links between circadian rhythms and psychiatric disease. Jager, et al. [29] investigated the behavioral changes and dopaminergic dysregulation in mice lacking the nuclear receptor. Chung, et al. [30] analyzed the impact of circadian nuclear receptor *rev-erba* on midbrain dopamine production and mood regulation. Ye, et al. [31] discuss *bmal1* inhibition mediated by cryptochrome and period proteins in the mammalian circadian clock. Fifel, et al. [32] showed how the daily and circadian rhythms were altered following dopamine depletion in *mptp*-treated non-human primates. Colwell [33] studied the link between neural activity and molecular oscillations.

Bedrosian, et al. [34] investigated the timing of light exposure affects mood and brain circuits. Huang, et al. [35] showed that Circadian modulation of dopamine levels and dopaminergic neuron development contributes to attention deficiency and hyperactive behavior. Lee, et al. [36] identified a novel circadian clock modulator controlling *bmal1* expression through a *ror/rev-erb*-response element-dependent mechanism. Takahashi [37] studied the transcriptional architecture of the mammalian circadian clock. Albrecht [38] studied the effect of molecular mechanisms in mood regulation involving the circadian clock. A comparison of macroscopic models for human circadian rhythms was conducted by Hannay, et al. [39]. Kim and Reed [40] developed a mathematical model involving circadian rhythms and dopamine.

This research aims to conduct a bifurcation analysis and perform multiobjective nonlinear model predictive control (MNLMP) calculations on the dopamine circadian rhythms model of Kim and Reed [40]. The bifurcation analysis reveals the existence of unwanted Hopf bifurcations that cause limit cycles. An activation factor is used to eliminate the Hopf bifurcations. The MNLMP calculations revealed spikes in the control profiles. These spikes are also eliminated using the same activation factor.

The paper is organized as follows. The dopamine circadian rhythms model of Kim and Reed [40] is first described. The bifurcation analysis and multiobjective nonlinear model predictive procedures are then described followed by the results and discussion. The conclusions are then presented.

### Dopamine circadian rhythms model

In the Dopamine Circadian model by Kin and Reed [40] the variables are  $X = [P_1, P_2, P_3, P_4, C, PC, PC_N, PN, C_N, BC, REV, ROR, S, TH, MAO, DRD3]$ .  $P_1, P_2, P_3, P_4$  represent the period proteins PER with 1 2 3 4 *i* phosphorylations in the cytosol. C represents the CRYPTOCHROME protein (CRY) in the cytosol. PC,  $PC_N, PN, C_N$  represent the PER-CRY protein dimer in the cytosol, the nuclear PER-CRY protein dimer that inhibits BMAL1-CLOCK, the nuclear PER, and the nuclear CRY; that inhibits transcription driven by BMAL1-CLOCK.  $BC, REV, ROR, S, TH, MAO, DRD3$  represent the BMAL1-CLOCK; a protein dimer that drives the transcription of core clock genes, the orphan nuclear receptor REV-ERB, the retinoic acid receptor-related orphan receptor, the BMAL1 circadian clock gene, Tyrosine hydroxylase which is a rate-limiting enzyme in dopamine synthesis, the Monoamine oxidase which catalyzes dopamine degradation and the Dopamine receptor.

Table 1 contains the description of the model variables. The model consists of 16 differential equations and has three linked parts. The first part is the core circadian clock that consists of a feedback loop containing BC,  $P_1, P_2, P_3, P_4$ , PC,  $PC_N, PN$ .

The second part is the secondary feedback loop involving REV, ROR, S, and BC that influences the core clock while the

Table 1: Description of Model Variables.

BC BMAL1-CLOCK	protein dimer that drives the transcription of core clock genes
$P_i$	PERIOD protein (PER) with <i>i</i> phosphorylations in the cytosol
C	CRYPTOCHROME protein in the cytosol
PC PER-CRY	PC PER-CRY protein dimer in the cytosol
PCN	nuclear PER-CRY protein dimer;
PN	nuclear PER
CN	nuclear CRY;
ROR	retinoic acid receptor-related orphan receptor
REV	orphan nuclear receptor
S	Bmal1; circadian clock gene
TH	Tyrosine hydroxylase
MAO	Monoamine oxidase (MAO);
DRD3	DRD3 Dopamine receptor D3



third part is the dopamine (DA synthesis the elements of which are REV, ROR, and DRD3. All concentrations are in nanomoles (nM) and all rates are in nanomoles per hour (nM/hr). More details can be found in the work of Kim and Reed [40].

The model equations include algebraic expressions that are used in time-dependent differential equations. The function  $f$  is defined as

$$f(x, y, z) = \frac{(x - y - z) - [(x - y - z)^2 + 4zx]^{1/2}}{2x} \tag{1}$$

While the other functions are

$$BC_{fr} = f(BC, PC_N, k_d) \tag{2}$$

$$R_S(S, REV) = \frac{\rho_S}{(1 + k_S(1 - f(S, REV, \varepsilon_S)))^{n_S}} \tag{3}$$

$$A_S(S, REV, ROR) = \alpha_S f(S, REV, \varepsilon_S) \left( \frac{ROR}{ROR + k_S} \right) \tag{4}$$

$$R_{th}(TH, REV) = \frac{\rho_{th}}{(1 + k_{th}(1 - f(S, REV, \varepsilon_{th})))^{n_{th}}} \tag{5}$$

$$A_{th}(TH, REV, ROR) = \alpha_{th} f(TH, REV, \varepsilon_{th}) \left( \frac{ROR}{ROR + k_{th}} \right) \tag{6}$$

$$R_{dr}(DRD3, REV) = \frac{\rho_{dr}}{(1 + k_{dr}(1 - f(DRD3, REV, \varepsilon_{dr})))^{n_{dr}}} \tag{7}$$

$$A_{dr}(DRD3, REV, ROR) = \alpha_{dr} f(DRD3, REV, \varepsilon_{dr}) \left( \frac{ROR}{ROR + k_{dr}} \right) \tag{8}$$

$$G_1(BC_{fr}) = \frac{(BC_{fr})^n}{(BC_{fr})^n + (k_{rev})^n} \tag{9}$$

$$G_2(BC_{fr}) = \frac{(BC_{fr})}{(BC_{fr}) + (k)} \tag{10}$$

$$F(C_N) = \frac{\rho_C}{(1 + k_C C_N)^{n_C}} \tag{11}$$

The differential equations are

$$\frac{dP_1}{dt} = r_1 F(C_N) BC_{fr} - r_2 P_1 \tag{12}$$

$$\frac{dP_2}{dt} = r_2 P_1 - r_3 P_2 \tag{13}$$

$$\frac{dP_3}{dt} = r_3 P_2 - r_4 P_3 \tag{14}$$

$$\frac{dP_4}{dt} = r_4 P_3 + m_C PC - d_4 P_4 - \tau_C P_4 C \tag{15}$$

$$\frac{dC}{dt} = r_5 F(C_N) BC_{fr} + m_C PC - d_5 C - \tau_C P_4 C \tag{16}$$

$$\frac{dPC}{dt} = \tau_C P_4 C - d_6 PC - m_C PC \tag{17}$$

$$\frac{dPC_N}{dt} = r_6 PC + \tau_N P_N C_N - d_7 PC_N - m PC_N \tag{18}$$

$$\frac{dP_N}{dt} = -\tau_N P_N C_N - d_P P_N + m PC_N \tag{19}$$

$$\frac{dC_N}{dt} = -\tau_N P_N C_N - d_C C_N + m PC_N \tag{20}$$

$$\frac{dBC}{dt} = \beta_{bc} S - d_{BC} BC \tag{21}$$

$$\frac{dREV}{dt} = r_{rev} G_1(BC_{fr}) F(C_N) - d_{rev} REV \tag{22}$$

$$\frac{dROR}{dt} = b_{ror} + r_{ror} G_2(BC_{fr}) F(C_N) - d_{ror} ROR \tag{23}$$

$$\frac{dS}{dt} = \beta + R_S(S, REV) + A_S(S, REV, ROR) - d_S S \tag{24}$$

$$\frac{dTH}{dt} = b_{th} + R_{th}(TH, REV) + A_{th}(TH, REV, ROR) - d_{th} TH \tag{25}$$

$$\frac{dMAO}{dt} = r_M F(C_N) BC_{fr} - d_m MAO \tag{26}$$

$$\frac{dDRD3}{dt} = b_{dr} + R_{dr}(DRD3, REV) + A_{dr}(DRD3, REV, ROR) - d_{dr} DRD3 \tag{27}$$

The parameters for the Core Circadian Clock are

$$K_d = 0.02; \rho_C = 3; k_C = 0.5; n_C = 3; r_1 = 5; r_2 = 0.45; r_3 = 0.45; r_4 = 0.45; m_C = 0.5; d_4 = 0.4; r_C = 0.5; r_5 = 5; d_5 = 0.1; d_6 = 0.12; r_6 = 0.75; d_7 = 0.2; \tau_n = 0.1; d_P = 0.25; d_C = 0.2; \beta_{bc} = 0.1; d_{bc} = 0.1; \xi = 2/3$$

The parameters for the secondary loop are

$$n = 2; k_{rev} = 0.2; k = 1.5; \rho_S = 1; k_S = 0.5; \varepsilon_S = 0; n_S = 5.3; \alpha_S = 3.7; r_{rev} = 1.5; d_{rev} = 0.5; b_{ror} = 0.1; r_{ror} = 1.8; d_{ror} = 0.25; \beta = 0.9; d_S = 3$$

The parameters for the equations of the dopamine (DA) elements are

$$\rho_{th} = 1; k_{th} = 10; \varepsilon_{th} = 0.4; \alpha_{th} = 1.23; k_{th} = 1; b_{th} = 0.85; d_{th} = 5.6; d_m = 0.016$$

$$\rho_{dr} = 1; k_{dr} = 10; \varepsilon_{dr} = 0.4; n_{dr} = 1; \alpha_{dr} = 0.53; b_{dr} = 0.3; d_{dr} = 3$$

**Numerical methods used**

**Bifurcation analysis:** Multiple steady-states and oscillatory behavior occur in various situations. Branch and Limit bifurcation points cause multiple steady-states while Hopf bifurcation points produce limit cycles. The MATLAB program MATCONT [41,42] is a commonly used software to locate limit points, branch points, and Hopf bifurcation points. Consider an ODE system

$$\dot{x} = f(x, \beta) \tag{28}$$

$x \in R^n$ . Defining the matrix A as

$$A = \begin{bmatrix} \frac{\partial f_1}{\partial x_1} & \frac{\partial f_1}{\partial x_2} & \frac{\partial f_1}{\partial x_3} & \frac{\partial f_1}{\partial x_4} & \dots & \frac{\partial f_1}{\partial x_n} & \frac{\partial f_1}{\partial \beta} \\ \frac{\partial f_2}{\partial x_1} & \frac{\partial f_2}{\partial x_2} & \frac{\partial f_2}{\partial x_3} & \frac{\partial f_2}{\partial x_4} & \dots & \frac{\partial f_2}{\partial x_n} & \frac{\partial f_2}{\partial \beta} \\ \dots & \dots & \dots & \dots & \dots & \dots & \dots \\ \frac{\partial f_n}{\partial x_1} & \frac{\partial f_n}{\partial x_2} & \frac{\partial f_n}{\partial x_3} & \frac{\partial f_n}{\partial x_4} & \dots & \frac{\partial f_n}{\partial x_n} & \frac{\partial f_n}{\partial \beta} \end{bmatrix} \tag{29}$$

$\beta$  is the bifurcation parameter. The matrix A can be written in a compact form as

$$A = [B \mid \partial f / \partial \beta] \tag{30}$$

The tangent at any point  $x$ ; ( $v = [v_1, v_2, v_3, v_4, \dots, v_{n+1}]$ ) must satisfy

$$Av = 0 \tag{31}$$

The matrix B must be singular at both limit and branch points. The  $n+1^{th}$  component of the tangent vector  $V_{n+1} = 0$  at a

limit point (LP) and for a branch point (BP) the matrix  $\begin{bmatrix} A \\ v^T \end{bmatrix}$  must be singular. At a Hopf bifurcation,

$$\det(2f_x(x, \beta) @ I_n) = 0 \tag{32}$$

@ indicates the bialternate product while  $I_n$  is the  $n$ -square identity matrix. Hopf bifurcations result in unwanted limit cycles (which in turn cause problems for optimization and control) and should be eliminated. Further details can be found in the works of Kuznetsov [43] and Govaerts [44].

**Multiobjective nonlinear model predictive control algorithm**

Flores Tlacuahuaz [45] first proposed the Multiobjective

nonlinear model predictive control method that does not involve weighting functions, nor does it impose additional constraints on the problem unlike the weighted function or the epsilon correction method [46]. For a set of ODE

$$\frac{dx}{dt} = F(x, u) \tag{33}$$

$$h(x, u) \leq 0 \quad x^L \leq x \leq x^U; \quad u^L \leq u \leq u^U$$

For a final time of  $t_f$  let  $p_j(t_f)$   $j=1,2,\dots,n$  be the variables that need to be optimized (maximized or minimized). Simultaneously,  $n$  the total number of variables that need to be optimized simultaneously. In this MNLMPCC method, dynamic optimization problems that independently minimize/maximize each variable  $p_j(t_f)$   $j=1,2,\dots,n$  are solved individually. The individual minimization/maximization of each  $p_j(t_f)$

$j=1,2,\dots,n$  will lead to the values  $p_j^*$ . Then the multiobjective

optimal control problem that will be solved is

$$\min \left( \sum_{j=1}^n (p_j(t_f) - p_j^*)^2 \right)$$

$$\text{subject to } \frac{dx}{dt} = F(x, u); \quad h(x, u) \leq 0 \tag{34}$$

$$x^L \leq x \leq x^U; \quad u^L \leq u \leq u^U$$

This will provide the control values for various times. The first obtained control value is implemented and the rest are ignored. The procedure is repeated until the implemented and the first obtained control values are the same or if the

Utopia point  $p_j(t_f) = p_j^*$ ; for all  $j$  from 1 to  $n$  is achieved.

The optimization package in Python, Pyomo [47], where the differential equations are automatically converted to algebraic equations will be used. The resulting optimization problem was solved using IPOPT [48]. The obtained solution is confirmed as a global solution with BARON [49]. To summarize the steps of the algorithm are as follows.

1. Minimize/maximize  $p_j(t_f)$   $j=1,2,\dots,n$ . This will lead to the value  $p_j^*$ .
2. Minimize  $\left( \sum_{j=1}^n (p_j(t_f) - p_j^*)^2 \right)$ . This will provide the control values for various times.
3. Implement the first obtained control values and discard the remaining.
4. The steps are repeated until there is an insignificant difference between the implemented and the first obtained value of the control variables or if the Utopia point is achieved.

**Results and discussion**

The Variables are ordered as

$X = [P_1, P_2, P_3, P_4, C, PC, PC_{NP}, PN, C_{NP}, BC, REV, ROR, S, TH, MAO, DRD_3]$ . Bifurcation analysis was performed using the MATLAB program MATCONT.  $d_s$  is the bifurcation parameter. The bifurcation analysis revealed the existence of two Hopf bifurcation points given by HA and HB in Figure 1. The variable values at both these bifurcation points are  $X = (0.668579 \ 0.668579 \ 0.668579 \ 0.369388 \ 2.216329 \ 0.6660230 \ 1.197233 \ 1.406020 \ 1.757524 \ 1.230547 \ 0.416188 \ 0.665301 \ 1.230547 \ 0.348979 \ 112.822706 \ 0.575163 \ 1.699851)$  and  $X = (0.944861 \ 0.944861 \ 0.944861 \ 0.482939 \ 2.897634 \ 1.128532 \ 2.379765 \ 2.243310 \ 2.804137 \ 3.868766 \ 0.515709 \ 0.723462 \ 3.868766 \ 0.646619 \ 159.445209 \ 1.411344 \ 0.713746)$ , respectively.

The limit cycles that occur at both these points are shown in Figures 2,3. When the bifurcation parameter  $d_s$  was modified to  $(d_s \tanh(d_s)) / 40$ ; both the Hopf bifurcation parameters disappeared. (Figure 4) Sridhar in 2024 [50] explained with several examples how the activation factor involving the tanh activation function where a bifurcation parameter  $u$  is replaced by  $(u \tanh u / \epsilon)$  successfully eliminates the limit cycle causing Hopf bifurcation points. Eliminating the Hopf bifurcation points in the dopamine circadian rhythms model using the tanh factor confirms the results [50].

DRD3 plays an important role in cognition. BC is the protein dimer that drives the transcription of core clock genes. TH (Tyrosine hydroxylase) is the rate-limiting enzyme in dopamine synthesis. MAO (Monoamine oxidase) catalyzes dopamine degradation. Hence, the MNL MPC aims to maximize the final value of the dopamine receptor (DRD3) and BC while minimizing the final values of MAO and TH.

The MNL MPC strategy described previously was used.  $d_s$  is the control variable.  $DRD3(t_f) + BC(t_f)$  was first maximized the resulted in a value of 107.1273. Then  $TH(t_f) + MAO(t_f)$  was minimized. This resulted in a value of 0.0969. The multiobjective optimal control problem involved the minimization of t

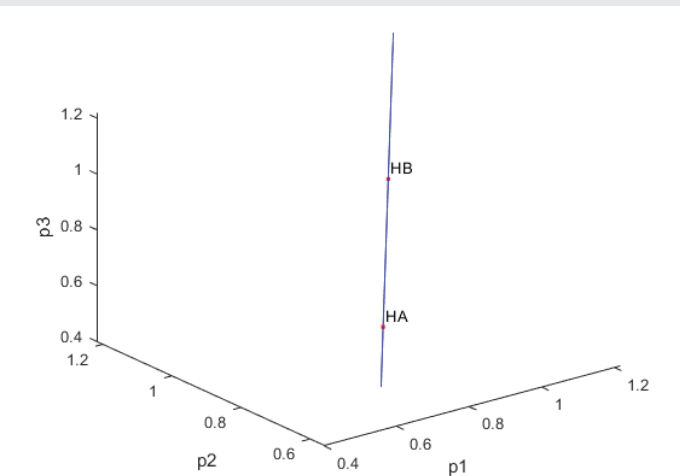


Figure 1: Two Hopf bifurcation Points HA and HB when tanh activation factor was not used.

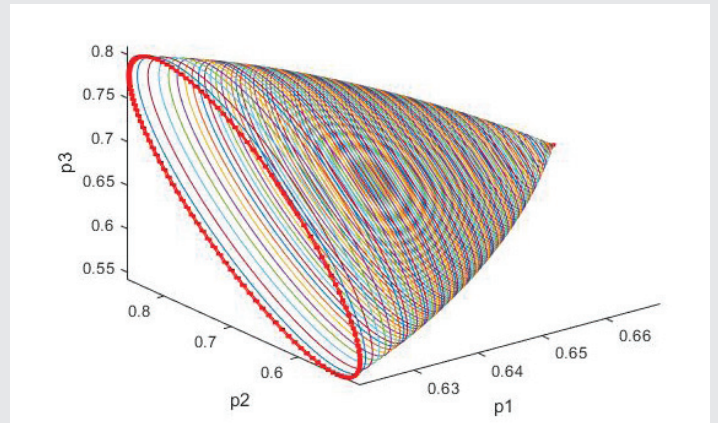


Figure 2: Limit cycle because of Hopf bifurcation point HA.

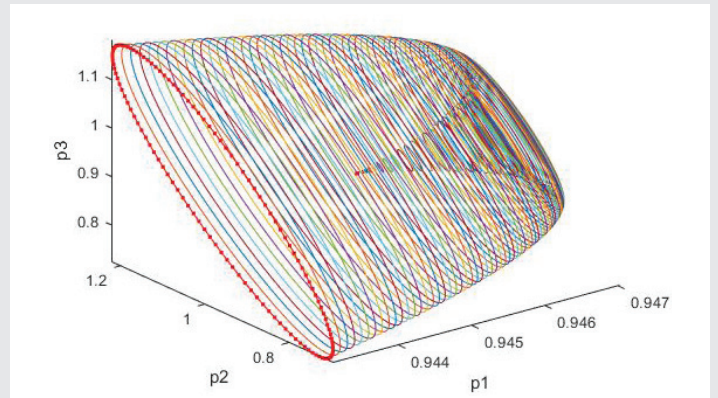


Figure 3: Limit cycle because of Hopf bifurcation point HB.

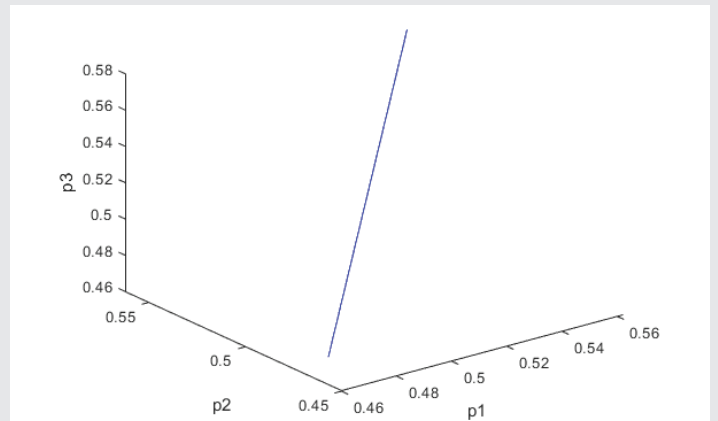


Figure 4: Both Hopf bifurcation points disappear because of the use of the activation factor involving the tanh function.

$$(DRD3(t_f) + BC(t_f) - 107.1273)^2 + (TH(t_f) + MAO(t_f) - 0.0969)^2$$

. The first obtained control value was implemented and the rest discarded until there was no difference between the implemented and the first obtained control value. This obtained value is referred to as the MNL MPC value.

The MNL MPC value obtained was  $d_s = 0.0326163$ . The resulting profiles are shown in Figures 5-7.

Figure 7 shows the  $d_s$  versus t profile that demonstrates

the existence of spikes. The tanh activation factor effectively eliminates spikes in optimal control profiles [51,52,53]. When the control variable  $d_s$  was modified to  $(d_s \tanh(d_s)) / 40$ ; and the MNLMPCC calculations were done again.

The maximization of  $DRD3(t_f) + BC(t_f)$  produced a value of 107.17.  $TH(t_f) + MAO(t_f)$  was then minimized and the value obtained was 0.3567. The multiobjective optimal control problem involved the minimization of  $(DRD3(t_f) + BC(t_f) - 107.17)^2 + (TH(t_f) + MAO(t_f) - 0.3567)^2$ . The first obtained control value was implemented and the rest discarded until there was no difference between the implemented and the first obtained control value. The MNLMPCC value obtained was  $d_s = 0.6731$ .

The resulting profiles are shown in Figures 8-10. Figure 10 shows the  $d_s$  versus  $t$  profile demonstrating that the spikes have been eliminated because of the tanh activation factor.

The multiobjective nonlinear model predictive control

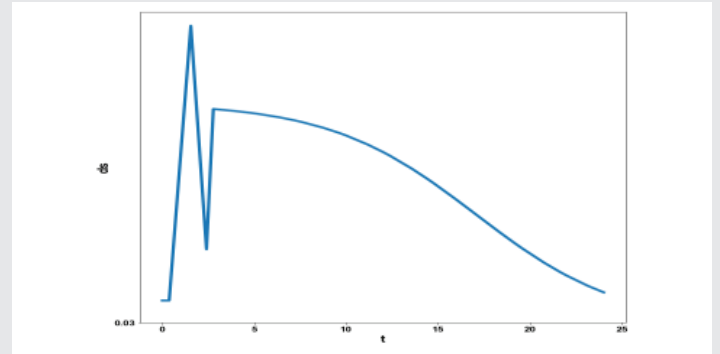


Figure 7:  $d_s$  profile when activation factor was not used in MNLMPCC calculation.

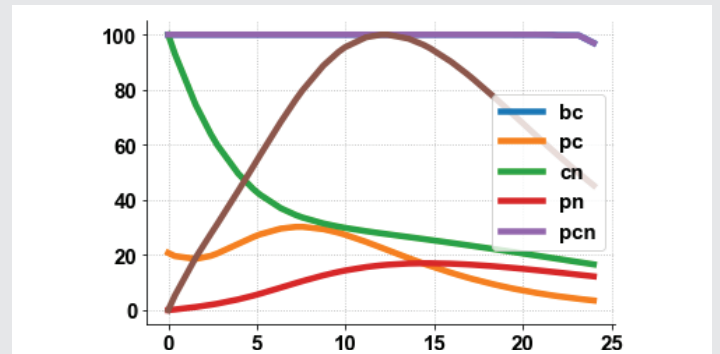


Figure 8: bc pc cn pn and pcn profiles when activation factor was used in MNLMPCC calculation.

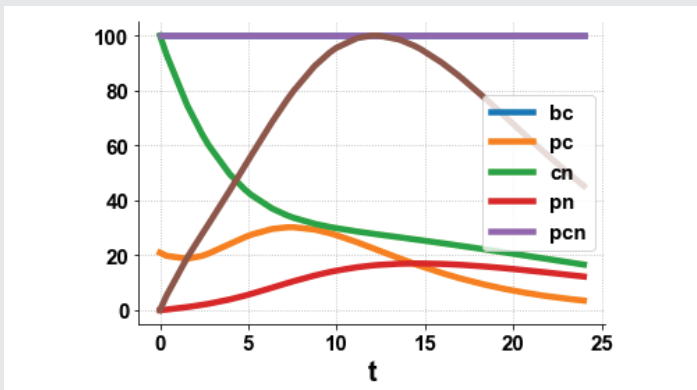


Figure 5: bc pc cn pn and pcn profiles when activation factor was not used in MNLMPCC calculation.

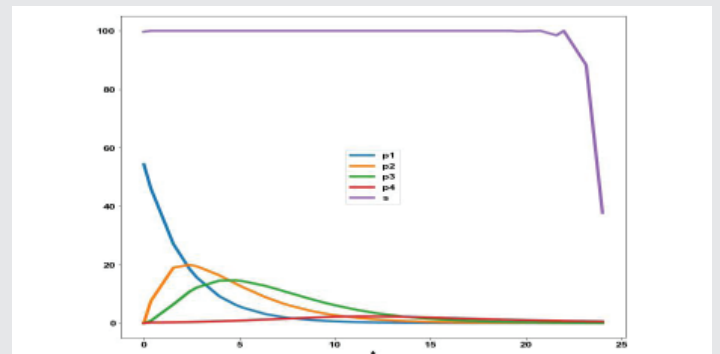


Figure 9:  $p_1, p_2, p_3, p_4, s$  profiles when activation factor was not used in MNLMPCC calculation.

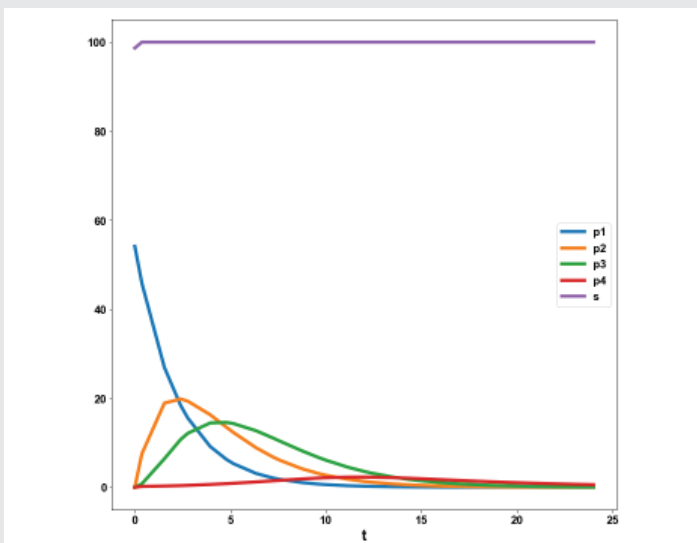


Figure 6:  $p_1, p_2, p_3, p_4, s$  profiles when activation factor was not used in MNLMPCC calculation.

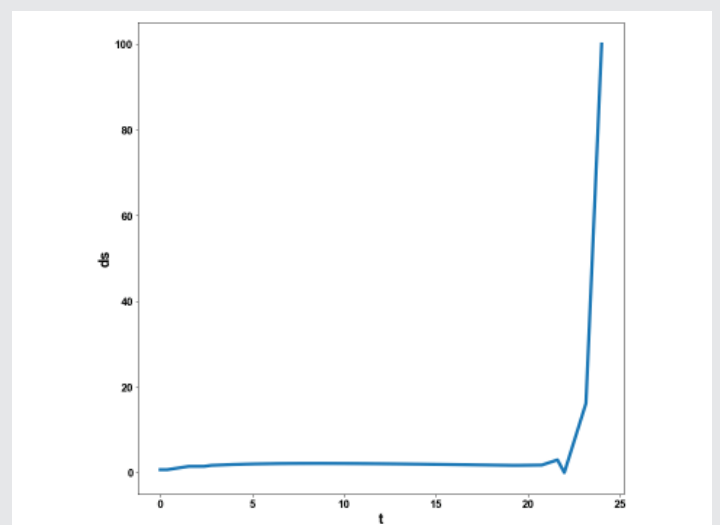


Figure 10:  $d_s$  profile when activation factor was used in MNLMPCC calculation.



is more rigorous than other methods that involve additional unnecessary constraints or equations [46]. The elimination of the Hopf bifurcations avoids the unnecessary limit cycles that may disrupt the circadian rhythm.

## Conclusions and future work

The dopamine circadian rhythms model is shown to have two Hopf bifurcations, which cause limit cycles that can disrupt the circadian rhythms. An activation factor involving the tanh function eliminates the limit cycle causing Hopf bifurcations. The high nonlinearity in the dopamine circadian rhythms model also produces spikes when multiobjective nonlinear model predictive calculations are performed. The same activation factor also eliminates the spikes in the control profiles. Future work will involve the performance of a combination of bifurcation analysis and Multiobjective nonlinear model predictive control calculations on more advanced Circadian rhythm models.

## Availability of data and material

All data used is presented in the paper.

## Competing interest

The author, Dr. Lakshmi N Sridhar has no conflict of interest.

## Authors' contributions

I am the only author and did all the work solely.

## Acknowledgement

Dr. Sridhar thanks Dr. Carlos Ramirez for encouraging him to write single-author papers.

## References

- Graybiel AM, Aosaki T, Flaherty AW, Kimura M. The basal ganglia in adaptive motor control. *Science*. 1994;265:1826–1831. Available from: <https://doi.org/10.1126/science.8091209>
- Vitaterna MH, Selby CP, Todo T, Niwa H, Thompson C, Fruechte EM, et al. Differential regulation of mammalian period genes and circadian rhythmicity by cryptochromes 1 and 2. *Proc Natl Acad Sci U S A*. 1999;96(21):12114–9. Available from: <https://doi.org/10.1073/pnas.96.21.12114>
- Van der Horst GTJ, Muijtjens M, Kobayashi K, Takano R, Kanno S-i, Takao M, et al. Mammalian cry1 and cry2 are essential for maintenance of circadian rhythms. *Nature*. 1999;398(6728):627–30. Available from: <https://www.nature.com/articles/19323>
- Strogatz SH. From kuramoto to crawford: exploring the onset of synchronization in populations of coupled oscillators. *Phys D*. 2000;143:1–20. Available from: [https://doi.org/10.1016/S0167-2789\(00\)00094-4](https://doi.org/10.1016/S0167-2789(00)00094-4)
- Shearman LP, Sriram S, Weaver DR, Maywood ES, Chaves I, Zheng B, et al. Interacting molecular loops in the mammalian circadian clock. *Science*. 2000;288(5468):1013–9. Available from: <https://doi.org/10.1126/science.288.5468.1013>
- Abarca C, Albrecht U, Spanagel R. Cocaine sensitization and reward are under the influence of circadian genes and rhythm. *Proc Natl Acad Sci USA*. 2002;99(13):9026–30. Available from: <https://doi.org/10.1073/pnas.142039099>
- Preitner N, Damiola F, Molina L-L, Zakany J, Duboule D, Albrecht U, et al. The orphan nuclear receptor rev-erba controls circadian transcription within the positive limb of the mammalian circadian oscillator. *Cell*. 2002;110:251–60. Available from: [https://doi.org/10.1016/S0092-8674\(02\)00825-5](https://doi.org/10.1016/S0092-8674(02)00825-5)
- Lotharius J, Brundin P. Pathogenesis of Parkinson's disease: dopamine vesicles and alpha-synuclein. *Nat Rev Neurosci*. 2002;3:932–42. Available from: <https://doi.org/10.1038/nrn983>
- Oleksiak M, Churchgill G, Crawford D. Variation in gene expression within and among natural populations. *Nat Genet*. 2002;32(2):261–6. Available from: <https://doi.org/10.1038/ng983>
- Boeuf S, Keijer J, Hal N, Klaus S. Individual variation of adipose gene expression and identification of covariate genes by cDNA microarrays. *Physiol Genomics*. 2002;11(1):31–6. Available from: <https://doi.org/10.1152/physiolgenomics.00051.2002>
- Forger DB, Peskin CS. A detailed predictive model of the mammalian circadian clock. *Proc Natl Acad Sci USA*. 2003;100(25):14806–11. Available from: <https://doi.org/10.1073/pnas.2036281100>
- Leloup J-C, Goldbeter A. Toward a detailed computational model for the mammalian circadian clock. *Proc Natl Acad Sci USA*. 2003;100(12):7051–6. Available from: <https://doi.org/10.1073/pnas.1132112100>
- Akashi M, Okamoto A, Tsuchiya Y, Todo T, Nishida E, Node K. A positive role for period in mammalian circadian gene expression. *Cell Rep*. 2014;7:1056–64. Available from: [https://www.cell.com/cell-reports/fulltext/S2211-1247\(14\)00282-4](https://www.cell.com/cell-reports/fulltext/S2211-1247(14)00282-4)
- Castaneda TR, Marquez de Prado B, Prieto D, Mora F. Circadian rhythms of dopamine, glutamate and gaba in the striatum and nucleus accumbens of the awake rat: modulation by light. *J Pineal Res*. 2004;36(3):177–85. Available from: <https://doi.org/10.1046/j.1600-079x.2003.00114.x>
- Kienast T, Heinz A. Dopamine in the diseased brain. *CNS Neurol Disord Drug Targets*. 2006;5:109–31. Available from: <https://doi.org/10.2174/187152706784111560>
- Sigal A, Milo R, Chen A, Gava-Zatorsky N, Klein Y, Liron Y, et al. Variability and memory of protein levels in human cells. *Nat Lett*. 2006;444:643–6. Available from: [https://ideas.repec.org/a/nat/nature/v444y2006i7119d10.1038\\_nature05316.html](https://ideas.repec.org/a/nat/nature/v444y2006i7119d10.1038_nature05316.html)
- Hong CI, Conrad ED, Tyson JJ. A proposal for robust temperature compensation of circadian rhythms. *Proc Natl Acad Sci U S A*. 2007;104(4):1195–200. Available from: <https://doi.org/10.1073/pnas.0601378104>
- McClung CA. Circadian genes, rhythms and the biology of mood disorders. *Pharmacol Ther*. 2007;114(2):222–32. Available from: <https://doi.org/10.1016/j.pharmthera.2007.02.003>
- Sleipness EP, Sorg BA, Jansen HT. Diurnal differences in dopamine transporter and tyrosine hydroxylase levels in rat brain: Dependence on the suprachiasmatic nucleus. *Brain Res*. 2007;1129:34–42. Available from: <https://doi.org/10.1016/j.brainres.2006.10.063>
- Hampp G, Ripperger JA, Houben T, Schmutz I, Blex C, Perreau-Lenz S, et al. Regulation of monoamine oxidase A by circadian-clock components implies clock influence on mood. *Curr Biol*. 2008;18:678–83. Available from: <https://doi.org/10.1016/j.cub.2008.04.012>
- Liu AC, Tran HG, Zhang EE, Priest AA, Welsh DK, Kay SA. Redundant function of rev-erba and  $\beta$  and non-essential role for bmal1 cycling in transcriptional regulation of intracellular circadian rhythms. *PLoS Genet*. 2008;4(2):1000023. Available from: <https://doi.org/10.1371/journal.pgen.1000023>
- Hood S, Cassidy P, Cossette M-P, Weigl Y, Verwey M, Robinson B, et al. Endogenous dopamine regulates the rhythm of expression of the clock protein per2 in the rat dorsal striatum via daily activation of d2 dopamine



- receptors. *J Neurosci.* 2010;30(42):14046–58.  
Available from: <https://doi.org/10.1523/jneurosci.2128-10.2010>
23. Ripperger JA, Jud C, Albrecht U. The daily rhythm of mice. *FEBS Lett.* 2011;585:1384–92.  
Available from: <https://doi.org/10.1016/j.febslet.2011.02.027>
24. Gravotta L, Gavrilu AM, Hood S, Amir S. Global depletion of dopamine using intracerebroventricular 6-hydroxydopamine injection disrupts normal circadian wheel-running patterns and period2 expression in the rat forebrain. *J Mol Neurosci.* 2011;45(2):162–71.  
Available from: <https://doi.org/10.1007/s12031-011-9520-8>
25. Bugge A, Feng D, Everett LJ, Briggs ER, Mullican SE, Wang F, et al. Rev-erba and rev-erb $\beta$  coordinately protect the circadian clock and normal metabolic function. *Genes Dev.* 2012;26:657–67.  
Available from: <https://doi.org/10.1101/gad.186858.112>
26. Solt LA, Wang Y, Banarjee S, Hughes T, Kojetin DJ, Lundasen T, et al. Regulation of circadian behavior and metabolism by synthetic rev-erb agonists. *Nature.* 2013;485(7396):62–8.  
Available from: <https://doi.org/10.1038/nature11030>
27. Ikeda E, Matsunaga N, Kakimoto K, Hamamura K, Hayashi A, Koyanagi S, et al. Molecular mechanism regulating 24-hour rhythm of dopamine d3 receptor expression in mouse ventral striatum. *Mol Pharmacol.* 2013;83:959–67.  
Available from: <https://doi.org/10.1124/mol.112.083535>
28. Karatsoreos IN. Links between circadian rhythms and psychiatric disease. *Front Behav Neurosci.* 2014;8(162):1–5.  
Available from: <https://doi.org/10.3389/fnbeh.2014.00162>
29. Jager J, O'Brien WT, Manlove J, Krizman EN, Fang B, Gerhart-Hines Z, et al. Behavioral changes and dopaminergic dysregulation in mice lacking the nuclear receptor rev-erba. *Mol Endocrinol.* 2014;28(4):490–8. Available from: <https://doi.org/10.1210/me.2013-1351>
30. Chung S, Lee EJ, Yun S, Choe HK, Park S-B, Son HJ, et al. Impact of circadian nuclear receptor rev-erba on midbrain dopamine production and mood regulation. *Cell.* 2014;157:858–68.  
Available from: <https://doi.org/10.1016/j.cell.2014.03.039>
31. Ye R, Selby CP, Chiou Y-Y, Ozkan-Dagliyan I, Gaddameedhi S, Sancar A. Dual modes of clock: bmal1 inhibition mediated by cryptochrome and period proteins in the mammalian circadian clock. *Genes Dev.* 2014;28:1989–98.  
Available from: <https://doi.org/10.1101/gad.249417.114>
32. Fifel K, Vezoli J, Dzahini K, Claustrat B, Leviel V, Kennedy H, et al. Alteration of daily and circadian rhythms following dopamine depletion in MPTP treated non-human primates. *PLoS ONE.* 2014;9(1):86240–86240. Available from: <https://doi.org/10.1371/journal.pone.0086240>
33. Colwell CS. Linking neural activity and molecular oscillations in the SCN. *Nat Rev Neurosci.* 2015;12(10):553–69.  
Available from: <https://doi.org/10.1038/nrn3086>
34. Bedrosian TA, Nelson RJ. Timing of light exposure affects mood and brain circuits. *Transl Psychiatry.* 2015;7(e1017):1–9.  
Available from: <https://doi.org/10.1038/tp.2016.262>
35. Huang J, Zhong Z, Wang M, Chen X, Tan Y, Zhang S, et al. Circadian modulation of dopamine levels and dopaminergic neuron development contributes to attention deficiency and hyperactive behavior. *J Neurosci.* 2015;35(6):2572–87.  
Available from: <https://doi.org/10.1523/JNEUROSCI.2551-14.2015>
36. Lee J, Lee S, Chung S, Park N, Son GH, An H, et al. Identification of a novel circadian clock modulator controlling BMAL1 expression through a ROR/REV-ERB-response element-dependent mechanism. *Biochem Biophys Res Commun.* 2016;469:580–6.  
Available from: <https://doi.org/10.1016/j.bbrc.2015.12.030>
37. Takahashi JS. Transcriptional architecture of the mammalian circadian clock. *Nat Rev Genet.* 2017;18(3):164–79.  
Available from: <https://doi.org/10.1038/nrg.2016.150>
38. Albrecht U. Molecular mechanisms in mood regulation involving the circadian clock. *Front Neurol.* 2017;8(30):1–6.  
Available from: <https://doi.org/10.3389/fneur.2017.00030>
39. Hannay KM, Booth V, Forger DB. Macroscopic models for human circadian rhythms. *J Biol Rhythm.* 2019;34(6):658–71.  
Available from: <https://doi.org/10.1177/0748730419878298>
40. Kim R, Reed MC. A mathematical model of circadian rhythms and dopamine. *Theor Biol Med Model.* 2021;18:8.  
Available from: <https://doi.org/10.1186/s12976-021-00139-w>
41. Dhooge A, Govaerts W, Kuznetsov AY. MATCONT: A Matlab package for numerical bifurcation analysis of ODEs. *ACM Trans Math Softw.* 2003;29(2):141–64. Available from: <https://lab.semi.ac.cn/download/0.28315849875964405.pdf>
42. Dhooge A, Govaerts W, Kuznetsov AY, Mestrom W, Riet AM. CL\_MATCONT: A continuation toolbox in Matlab. Available from: [https://www.maths.kuleuven.be/analysis/na/software/CL\\_MATCONT/](https://www.maths.kuleuven.be/analysis/na/software/CL_MATCONT/)
43. Kuznetsov YA. Elements of applied bifurcation theory. New York: Springer; 1998.
44. Govaerts WJ. Numerical Methods for Bifurcations of Dynamical Equilibria. Philadelphia: SIAM; 2000. Available from: <https://pubs.siam.org/doi/pdf/10.1137/1.9780898719543.fm>
45. Flores-Tlacuahuac A, Morales P, Rivalero Toledo M. Multiobjective nonlinear model predictive control of a class of chemical reactors. *Ind Eng Chem Res.* 2012;51(14):5891–9. Available from: <http://dx.doi.org/10.1021/ie201742e>
46. Miettinen KM. Nonlinear Multiobjective Optimization. Kluwer International Series; 1999. Available from: [https://books.google.co.in/books/about/Nonlinear\\_Multiobjective\\_Optimization.html?id=ha\\_zLdNtXSMC&redir\\_esc=y](https://books.google.co.in/books/about/Nonlinear_Multiobjective_Optimization.html?id=ha_zLdNtXSMC&redir_esc=y)
47. Hart WE, Laird CD, Watson JP, Woodruff DL, Hackedbeil GA, Nicholson BL, et al. Pyomo – Optimization Modeling in Python. 2nd ed. Vol. 67. Springer; 2017. Available from: <https://f.openpdfs.org/E315vrGE5Yy.pdf>
48. Wächter A, Biegler L. On the implementation of an interior-point filter line-search algorithm for large-scale nonlinear programming. *Math Program.* 2006;106:25–57. Available from: <https://doi.org/10.1007/s10107-004-0559-y>
49. Tawarmalani M, Sahinidis NV. A polyhedral branch-and-cut approach to global optimization. *Math Program.* 2005;103(2):225–49. Available from: <http://dx.doi.org/10.1007/s10107-005-0581-8>
50. Sridhar LN. Elimination of oscillation causing Hopf bifurcations in engineering problems. *J Appl Math.* 2024;2(4):1826.  
Available from: <https://doi.org/10.59400/jam1826>
51. Sridhar LN. Multiobjective nonlinear model predictive control of diabetes models considering the effects of insulin and exercise. *Arch Clin Med Microbiol.* 2023;2(2):23–32. Available from: <https://www.opastpublishers.com/open-access-articles/multi-objective-nonlinear-model-predictive-control-of-diabetes-models-considering-the-effects-of-insulin-and-exercise.pdf>
52. Sridhar LN. Multiobjective nonlinear model predictive control of microalgal culture processes. *J Oil Gas Res Rev.* 2023;3(2):84–98. Available from: <https://www.opastpublishers.com/peer-review/multiobjective-nonlinear-model-predictive-control-of-microalgal-culture-processes-6595.html>
53. Sridhar LN. Bifurcation analysis and optimal control of the tumor-macrophage interactions. *Biomed J Sci Tech Res.* 2023;53(5):BJSTR.MS.ID.008470. Available from: <http://dx.doi.org/10.26717/BJSTR.2023.53.008470>